Mining of co-expression genes in response to cold stress at maize (*Zea mays* L.) germination and sprouting stages by weighted gene co-expression networks analysis

Chuangye Shi[1,2], Jing Dong[2], Chunxiao Zhang[2], Liquan Sun[1], Fengxue Jin[2], Xiaohui Zhou[2], Xueyan Liu[2], Weilin Wu[1] and Xiaohui Li[2]

[1] Agricultural College, Yanbian University, Yanji, Jilin Province, China
[2] Maize Research Institute, Jilin Academy of Agricultural Sciences, Gongzhuling, Jilin Province, China

ABSTRACT

Background: Maize (*Zea mays* L.) is one of the main agricultural crops with the largest yield and acreage worldwide. Maize at the germination and sprouting stages are highly sensitive to low-temperatures, especially in high-latitude and high-altitude regions. Low-temperature damage in early spring presents a major meteorological disaster in maize, severely affecting plant growth and maize yield. Therefore, mining genes tolerant to low temperatures is crucial. We aimed to analyze differential gene expression and construct co-expression networks in maize under low temperatures.

Methods: Inbred lines, Zhongxi 091/O2 and Chang 7-2, are tolerant and sensitive to low temperatures at the germination and sprouting stages, respectively. We grew these lines at 10 °C and 2 °C at the germination and sprouting stages, respectively. Samples were taken at five time points (0, 6, 12, 24, and 36 h) during the two stages, and transcriptome sequencing was performed. The analyses were conducted using weighted gene co-expression networks analysis (WGCNA), Gene Ontology (GO), the Kyoto Encyclopedia of Genes and Genomes (KEGG), and gene co-expression networks.

Results: WGCNA was used to construct co-expression networks at two stages, resulting in six and nine co-expression modules, respectively. Two modules at the germination stage (blue and yellow) and two modules at the sprouting stage (turquoise and magenta) were identified. These were significantly associated ($p < 0.01$) with tolerance at low temperature. The differentially expressed genes (DEGs) in the four modules revealed entries related to hormone and oxygen-containing compound responses by GO functional enrichment. Among the four modules, DEGs from three modules were all significantly enriched in the MAPK signaling pathway. Based on the connectivity, the top 50 genes for each module were selected to construct a protein interaction network. Seven genes have been proven to be involved in the response to low-temperature stress.

Conclusion: WGCNA revealed the differences in the response patterns of genes to low-temperature stress between tolerant and sensitive lines at different time points. Seven genes involved in low-temperature stress were functionally annotated. This finding suggests that WGCNA is a viable approach for gene mining. The current

findings provide experimental support for further investigation of the molecular mechanisms underlying tolerance to low temperatures in maize.

INTRODUCTION

Maize (*Zea mays* L.) is a major food, economic and feed crop worldwide (*Wang et al., 2020*). Due to its origin in tropical and subtropical regions, the growth and development of maize are highly sensitive to low-temperatures (*Greaves, 1996*). When planting in high latitude or high-altitude areas, the sudden low-temperature damage at the germination and sprouting stages can lead to cell membrane disorders, protein denaturation, metabolic dysfunction, and changes in oxidative defense and osmotic pressure, further resulting in irreversible damage to cells and tissues (*Allen & Ort, 2001*; *Hussain et al., 2018*; *Nguyen et al., 2009*). This not only reduces seed germination rates and seedling vigor, but also increases the chances of soil bacteria infecting maize (*Juurakko, Cenzo & Walker, 2021*). Hence, identifying genes capable of enhancing cold tolerance is crucial for low-temperature adaptation, ultimately ensuring the yield stability.

There have been some reports on gene mining tolerant to low-temperature stress in maize. Low-temperature stress induces the over-expression of four genes (*ZmDREB1A*, *ZmDREB2A*, *ZmDBP3*, and *ZmDBP4*), which enhances cold tolerance in maize (*Qin et al., 2004*). *ZmICE1* directly regulates the expression of *DREB1*. Natural variations in the *ZmICE1* promoter affect the binding affinity with the transcriptional activator *ZmMYB39*, which is a positive regulator of cold tolerance in maize. *ZmMYB39* results in varying levels of *ZmICE1* transcription and cold tolerance among inbred lines (*Jiang et al., 2022*). *ZmMYB31* reduces ion leakage, ROS levels, and low-temperature photo inhibition by positively regulating the expression of genes related to low-temperature stress, thereby enhancing cold tolerance (*Li et al., 2019*). In maize leaves, *ZmMPK5* was found to be involved in plant recovery from low temperature stress (*Berberich, Sano & Kusano, 1999*). *Kong et al. (2011)* isolated the group C MAPKK gene *ZmMKK4* from the root system of the cultivar Zhengdan958 and found that the expression of the *ZmMKK4* transcript was up-regulated due to low-temperature exposure. A recent study identified a novel cold regulation pathway in maize, *ZmMPK8-ZmRR1-ZmDREB1.10/ZmCesA2*. *ZmRR1* accumulates and induces the expression of *ZmDREB1s* and *ZmCesAs*, thereby enhancing cold tolerance. *ZmMPK8* is a negative regulator of cold tolerance that interacts with *ZmRR1* and phosphorylates *ZmRR1* at Ser15. A natural variation of *ZmRR1* with a 45-bp deletion that encompasses Ser15 prevents its phosphorylation by *ZmMPK8* (*Zeng et al., 2021*).

With the rapid development of high-throughput sequencing technologies, large amounts of sequencing data have been generated. WGCNA is based on transcriptome sequencing data. According to the difference in gene expression level, the genes are divided

into different categories. If the gene expression patterns are similar, they are divided into the same module, the saliency module related to the research trait is selected, and the key genes in the module are screened. Since *Langfelder & Horvath (2008)* proposed WGCNA, several key genes have been identified by this method, which are relevant to plant phenotypic traits, responses to biotic or abiotic stresses, and other aspects. *Zhang & Horvath (2005)* found 13 modules significantly correlated with corn kernel weight, with a correlation range of −0.87 to 0.89. *Yu et al. (2023)* used B144 (cold stress tolerant) and Q319 (cold stress sensitive) as experimental lines and identified four specific modules (deep orange, green-yellow, light yellow and purple) related to low-temperature tolerance at the maize seedling stage by WGCNA. *Wang et al. (2024)* identified five hub genes directly related to salt response from two alfalfa (*Medicago sativa* L) varieties with different resistances by WGCNA. *Zhao et al. (2024)* screened 11 co-expression modules closely related to cold stress resistance in quinoa (*Chenopodium quinoa* Wild.) seedlings and identified four important transcription factors involved in resisting cold stress from two of the modules. *Liang et al. (2022)* found four hub genes involved in Ca^{2+} transport in maize in response to salt stress. *Zhao et al. (2023)* determined 19 and 49 hub genes that regulated maize mesocotyl and coleoptile elongation plasticity under different light spectral quality stimulation.

We aimed to conduct differential expression analysis of transcriptome data of maize subjected to the 10 °C-germination stage and 2 °C-sprouting stage using antagonistic and sensory lines at different times. WGCNA was used to construct gene co-expression networks, linking gene expression modules with cryogenic treatments. Enrichment analysis was conducted to explore the function of differentially expressed core gene co-expression networks at the germination and sprouting stage of maize under low-temperature stress, which provided new clues and insights for further research on the molecular mechanism of maize low temperature stress.

MATERIALS AND METHODS

Experimental lines and treatments

In this experiment, different degrees of cold treatment were applied at two maize germination stages. The maize inbred lines Zhongxi 091/O2 and Chang 7-2 were subjected to RNA sequencing, which carried out by the Maize Research Institute of the Jilin Academy of Agricultural Sciences in Jilin, China. The maize inbred lines Zhongxi 091/O2 and Chang 7-2 were found to be resistant (R) and susceptible (S) (*Liu et al., 2021*) to cold stress at the germination and sprouting stages in previous studies, respectively. The identification data of the two lines are detailed in Fig. S1.

Germination stage: 200 plump seeds were selected and disinfected with 0.1% $HgCl_2$ for 10 min. The seeds were soaked at 25 °C for 12 h and then subjected to low-temperature treatment at 10 °C. The seeds were placed on a disinfected culture dish covered with a moist sponge and filter paper at a density of 20 seeds per dish. The dishes were placed separately in a smart light incubator (10 °C, 24 h dark culture, and 60% humidity). Samples were collected at five time intervals (0, 6, 12, 24, and 36 h), and several neatly germinating seeds were randomly selected. The embryos were dissected using a dissecting needle and

weighed to a total weight of 0.6 g. The experiment was repeated three times to ensure accuracy.

Sprouting stage: 500 plump seeds were selected and disinfected with 0.1% $HgCl_2$ for 10 min. The seeds were placed on a sterilized culture dish covered with a moist sponge and filter paper at a density of 20 seeds per dish. The dishes were placed in a smart light incubator for germination (25 °C, 24 h dark culture, and 60% humidity). When the sprouts were approximately 4 cm long, 100 seedlings of the same growth size were selected and subjected to low-temperature treatment at 2 °C. The samples were collected at five intervals (0, 6, 12, 24, and 36 h) and several seeds with the same sprout lengths were randomly selected. The seedlings were cut into cubes and weighed for a total weight of 0.6 g. The experiment was repeated three times to ensure accuracy.

The total RNA of maize at the germination and sprouting stages was extracted using the polysaccharide polyphenol plant total RNA extraction kit (Exp.01032020, stored at RT) of the Shanghai Pudi Biotechnology Co., Ltd. After purification, the ends were repaired, base A was added to the 3′ end, and then the sequencing adapter sequence was added. The target size fragment after gel electrophoresis was recovered, the library required for sequencing was amplified by PCR, and the sequencing was completed using an Illumina HiSeq™ 2000 sequencer.

Clustering analysis and functional enrichment of module genes

Gene co-expression network analysis was performed using the WGCNA package in R software (https://cran.r-project.org/web/packages/WGCNA/index.html). To ensure compliance with scale-free network distributions, for WGCNA, the appropriate weighting coefficient β must be selected. The value of coefficient β was estimated using the pick Soft Threshold function in the WGCNA package. First, the β = 1–30 was set to calculate the corresponding correlation coefficient and mean gene connectivity. The selection criterion of β is to ensure that the square of the correlation coefficient is as close as possible to 0.8, while also preserving a sufficient level of gene connectivity. The dynamic tree cut method was used to identify the co-expression module. The Automatic Network Builder Block-wise Module was used to build the network. Here, the minimum module size was 30, merge Cut Height = 0.25 merged the modules with a similarity of 0.75, and other parameters were set by default. To obtain the biological functions and signaling pathways involved in each module, genes in each module were subjected to GO analysis (http://systemsbiology.cau.edu.cn/agriGOv2/index.php) and KEGG analysis. The R package was then used to plot and display the results. The threshold for the GO term and the KEGG pathway was set as $p < 0.05$.

Weighted gene co-expression network analysis and gene network visualization

The gene co-expression network obtained from WGCNA was processed, and Cytoscape V3.6.1 was used to screen hub genes and visualize their network. Each node in the network represents a gene, and the edges represent the relationships between genes.

Real-time quantitative reverse transcription PCR (qRT-PCR) verification

Ten cold tolerance-related genes were randomly selected for qRT-PCR analysis. Total RNA was extracted from maize during the germination and sprouting stages at low temperatures using a Polysaccharide Polyphenol Plant Total RNA Extraction Kit (Shanghai Pudi Biotechnology Company, Shanghai, China). Reverse transcription was performed using the TaKaRa Reverse Transcriptase M-MLV (RNase H) reverse transcription kit (TaKaRa Bio Inc., Shiga, Japan). qRT-PCR was performed on a Quant Studio six and seven real-time fluorescence quantitative PCR instrument (Applied Biosystems, Waltham, MA, USA) using SYBR® Green Real-time PCR Master Mix (Toyobo, Osaka, Japan), following the manufacturer's instructions. The reaction conditions were as follows: 95 °C for 5 min, 95 °C for 15 s, 58 °C for 30 s, and 70 °C for 30 s, for a total of 35 cycles. Specific primers were designed using Primer 5.0 software and are listed in Table 1 with corn UBI as the internal reference gene. Gene expression levels were calculated using the $2^{-\Delta\Delta CT}$ method, where ΔCT refers to the difference of the CT value between the target and the internal reference gene (*Livak & Schmittgen, 2001*).

RESULTS

RNA sequencing

A total of 230.4 and 228.3 Gb raw readings were obtained from 60 samples (2 varieties × 5 time intervals × 3 replicates) at the germination and sprouting stages, respectively. After filtering, 1,544,300,100 and 1,531,483,946 clean reads were obtained, with a Q30 percentage above 95.00%. The percentage of GC ranged from 54.04% to 57.35%, indicating that all experimental samples were highly reliable in terms of collection and sequencing results. The statistical power of this experimental design, calculated using RNA-Seq Power, was 0.84. To verify the effectiveness of cold stress treatment, the reported marker genes involved in cold stress were evaluated for their expression patterns before and after cold stress treatment, and the results showed that with increasing cold stress duration, the expression of *ZmG6PDH5* (*LOC100383421*) increased and that of *ZmDREB1A* (*LOC103647602*) decreased, reaching the lowest value at 24 h. The results of the RNA-seq data were similar to previously reported results, indicating that the cold stress treatment carried out in this study was effective and further verified the reliability of the RNA-seq data (Fig. 1).

Principal coordinates analysis of cold stress

Principal coordinates analysis (PCA) was performed to explore the correlation between sample processing methods. In the PCA of cold stress at the two stages, the first principal coordinate primarily explained the difference in stage expression and had a large contribution, accounting for 62.96% of the total variance. This indicates that the germination and sprouting stage of stress should be analyzed separately when using WGCNA to construct a gene expression network to avoid stage differences in the stress treatment (Fig. 2A).

Table 1 Genes and primer pairs for fluorescence quantitative PCR.

Gene ID	Primer sequence	Description
Zm00001d034099	ATGTTGATGCCCAAAGACC	Ferredoxin–NADP reductase leaf isozyme 1 chloroplastic
	AGGAAGAGCCAGCCCAGA	
Zm00001d022125	AAGAGGAGATTCGGAGTGG	Exportin-T
	TTAAAGCCCTTGCTGACC	
Zm00001d045557	TGCCTGACTCGATACGCC	Putative cellulose synthase-like family protein
	GCTCCAGCCTTCTTGTTGTG	
Zm00001d039718	ACCTCTTCCGCTCCTTCCTC	Mini-chromosome maintenance complex-binding protein
	TCACCTTCCTTCGGCTTCTT	
Zm00001d003601	ATCATTGGCATCGGGAGT	Auxin response factor 6
	GCTTTGGGATTCAAGAGGT	
Zm00001d028401	TGGACGGCGTACCTCA	Auxin transporter-like protein 3
	GTGCCCTCCGAAAGTG	
Zm00001d030310	CAGCACGCACAAGCAGG	auxin import carrier1
	CCGAACGCCCAGTAGGA	
Zm00001d010863	TTCATTGGCTCAGTCTATTTC	Protein transport inhibitor response 1
	CTTCCTGTTCCGAGTTCTAC	
Zm00001d002533	AGCCAGGCGAGCCAACA	Abscisic acid receptor PYL9
	CCGACGAGACCCACCATCT	
Zm00001d047705	TGACCACCGTCCACCCGTCC	Cyclase/dehydrase family protein
	GGCTGCGAGTGCGAGCTTCT	
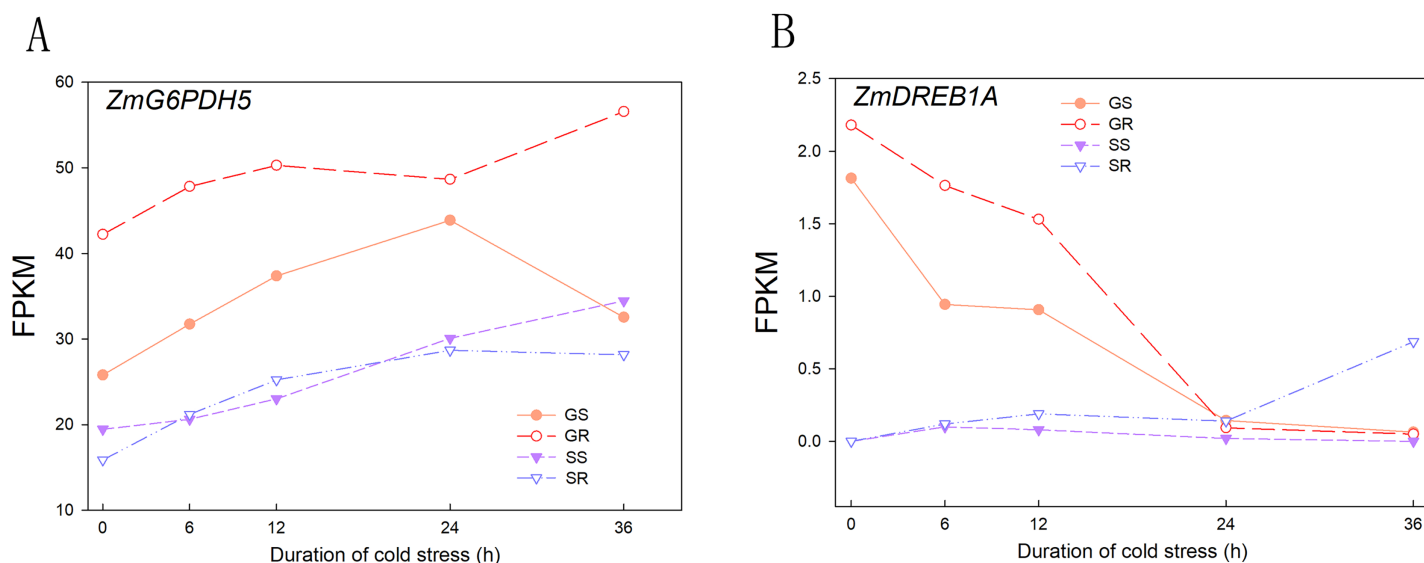
Figure 1 Expression patterns of cold stress response marker genes. (A) Expression of *ZmG6PDH5* gene in GR, GS, SR and SS. (B) Expression of *ZmDREB1A* gene in GR, GS, SR and SS. Abbreviations: Resistant inbred lines at the Germination stage (GR); Susceptible inbred lines at the Germination stage (GS); Resistant inbred lines at the Sprouting stage (SR); Susceptible inbred lines at the Sprouting stage (SS).

Full-size 🖼 DOI: 10.7717/peerj.19124/fig-1
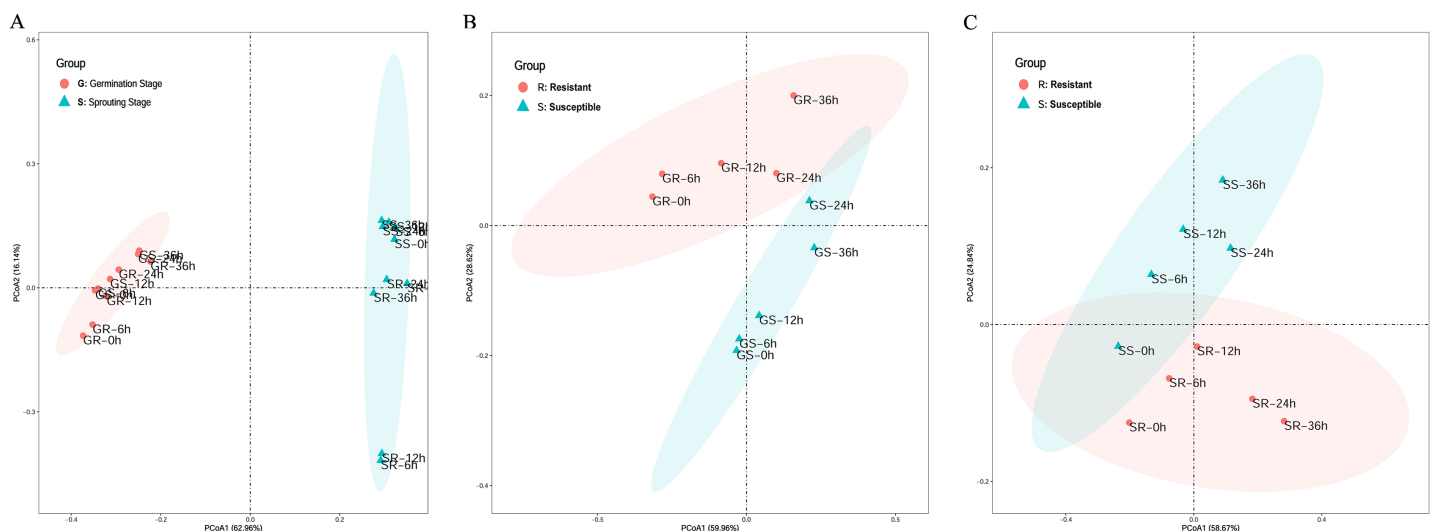
Figure 2 **Principle component analysis of cold stress.** (A) Clustering of cold-resistant inbred line Zhongxi 091/O2 (R) and cold-sensitive inbred line Chang 7-2 (S). (B, C) Clustering of cold-resistant inbred line Zhongxi 091/O2 (R) and cold-sensitive inbred line Chang 7-2 (S) during the germination (G) and sprouting (S) stages. Abbreviations: Resistant inbred lines at the Germination stage (GR); Susceptible inbred lines at the Germination stage (GS); Resistant inbred lines at the Sprouting stage (SR); Susceptible inbred lines at the Sprouting stage (SS).

Full-size 🖼 DOI: 10.7717/peerj.19124/fig-2

In the PCA of cold stress of the lines at the germination stage, the first principal coordinate primarily explained the differences in line expression, accounting for 59.96% of the total variance. In the PCA of cold stress of the lines at the sprouting stage, the first principal coordinate primarily explained the difference in line expression and had a large contribution, accounting for 58.67% of the total variance. This indicates that when using WGCNA to construct a gene expression network, the R and S lines under stress at the germination and sprouting stage should be analyzed separately to avoid line differences in the stress treatment (Figs. 2B and 2C).

Differentially expressed genes analysis

There were 546 genes that responded at the germination and sprouting stages of both lines (Fig. 3A). A total of 14,384, 7,301, 10,295 and 10,799 DEGs were observed in Resistant inbred lines at the Germination stage (GR), Susceptible inbred lines at the Germination stage (GS), Resistant inbred lines at the Sprouting stage (SR), and Susceptible inbred lines at the Sprouting stage (SS) within 36 h of low temperature stress, respectively. The number of DEGs for the R and S lines both exhibited an increasing trend with the extension of stress duration, except for SS. SS decreased after reaching its maximum value at 24 h, while the other three treatments reached their maximum at 36 h (Fig. 3B). Compared to the sensitive line Chang 7-2 (18,100), a greater number of genes were involved in Zhongxi 091/O2 (24,679). Notably, the number of up-regulated genes (14,182) was significantly higher than that of down-regulated genes (10,497) in Zhongxi 091/O2. Conversely, there was no significant difference in the number of up-regulated (9,449) and down-regulated genes (8,651) in Chang 7-2 (Figs. 3C and 3D).

A

B

C

D
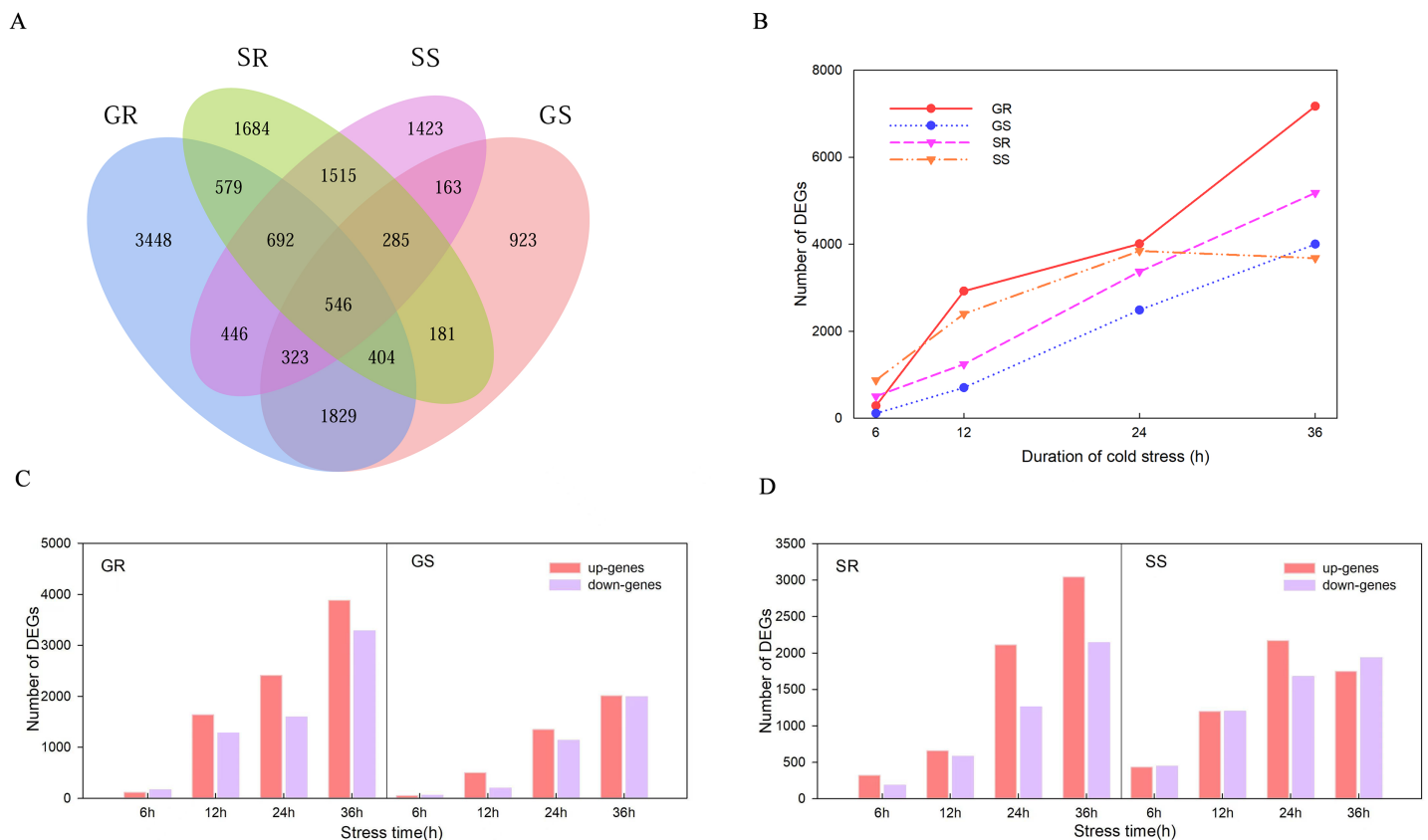
Figure 3 Differentially expressed genes (DEGs) analysis. (A) Venn diagram of DEGs during the germination (G) and sprouting (S) stages of Zhongxi 091/O2 (R) and Chang 7-2 (S). (B) Trend of the number of DEGs changing with treatment time. (C, D) The number of up-regulated and down-regulated DEGs at each time point. Abbreviations: Resistant inbred lines at the Germination stage (GR); Susceptible inbred lines at the Germination stage (GS); Resistant inbred lines at the Sprouting stage (SR); Susceptible inbred lines at the Sprouting stage (SS).

Full-size 🖼 DOI: 10.7717/peerj.19124/fig-3

WGCNA analysis

The weight values were calculated, and the appropriate soft threshold was selected to ensure that the co-expression network followed a scale-free network distribution. The results showed that the optimal soft threshold values were $\beta = 20$ at the germination stage and $\beta = 15$ at the sprouting stage. This was further used to construct a co-expression network (Fig. S2).

First, cluster analysis was carried out according to the expression of genes, and genes with a high degree of clustering were divided into a module. Then, the dynamic cleavage method was used to identify the co-expression modules. Different modules are indicated by different colors, and grey represents the genes not assigned to any module (Fig. 4). Six modules were obtained at the germination stage, among which the turquoise module contained the greatest number of genes (3,635) and the red contained the least number (43). At the sprouting stage, nine modules were formed. The turquoise module had 2,668 genes, whereas the magenta and pink had only 202 genes each (Figs. 4A and 4B).

Shi et al. (2025), *PeerJ*, DOI 10.7717/peerj.19124

8/20
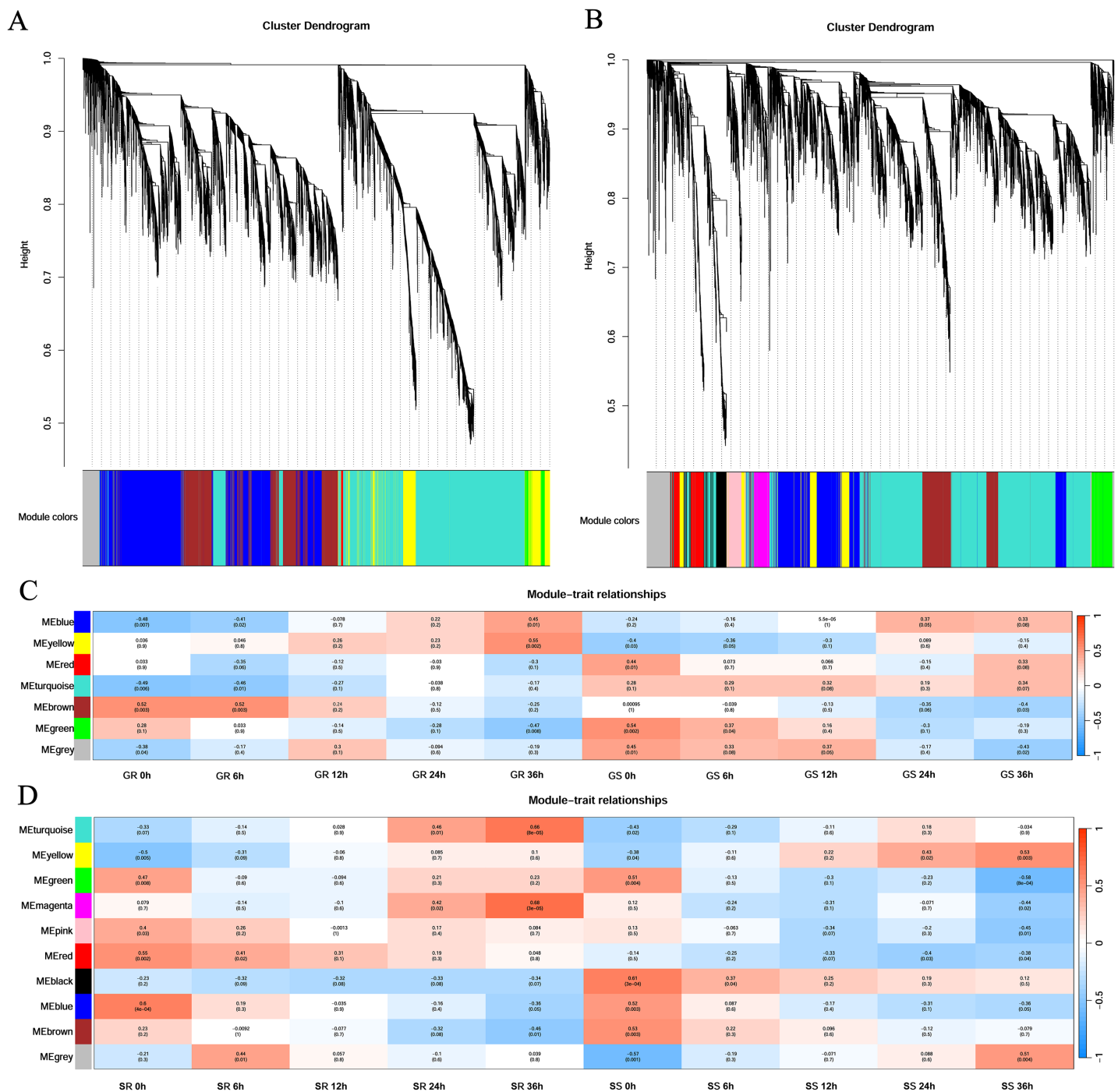
Figure 4 Gene clustering tree and module cutting, module-trait-relationship heatmap. (A, B) Gene clustering trees and module partitioning at germination (G) and sprouting (S) stages. (C, D) Module-trait-relationship heatmap at germination (G) and sprouting (S) stages. Abbreviations: Resistant inbred lines at the Germination stage (GR); Susceptible inbred lines at the Germination stage (GS); Resistant inbred lines at the Sprouting stage (SR); Susceptible inbred lines at the Sprouting stage (SS). Full-size 🖻 DOI: 10.7717/peerj.19124/fig-4

At the germination stage, the correlation of the blue module with stress duration changed from significantly negative to significantly positive and was the most significant in Zhongxi 091/O2 at 36 h (r = 0.45, p = 0.01). A significantly positive correlation was

observed between the yellow module and stress duration in Zhongxi 091/O2, which reached a maximum at 36 h ($r = 0.55$, $p = 0.002$), whereas Chang 7-2 showed no significant correlation with stress duration (Fig. 4C).

At the sprouting stage, significantly positive correlations between the turquoise and magenta modules and stress duration in Zhongxi 091/O2 were observed, which reached a maximum at 36 h ($r = 0.66$, $p < 0.001$; $r = 0.68$, $p < 0.001$). Finally, we determined that the blue and yellow modules at the germination stage and the turquoise and magenta modules at the sprouting stage were maize low-temperature-specific modules (Fig. 4D).

## Enrichment analysis of specific modules under low-temperature stress

To investigate gene function within specific modules under low-temperature stress, the blue and yellow modules at the germination stage and the turquoise and magenta modules at the sprouting stage were annotated. All four modules were enriched in the response to hormone (GO:0009725) and oxygen-containing compounds (GO:1901700).

In the blue module, the genes were mainly enriched in the following: biological processes such as plant organ development (GO:0099402), developmental processes involved in reproduction (GO:0003006), and post-embryonic development (GO:0009791); molecular functions such as transcription factor activity, sequence-specific DNA binding (GO:0003700), nucleic acid binding transcription factor activity (GO:0001071), DNA binding (GO:0003677), and 2-alkenal reductase (NAD(P)$^+$) activity (GO:0032440); and cellular components such as DNA packaging complex (GO:0044815), organelle membrane (GO:0031090), and plasma membrane (GO:0005886) (Fig. 5A). In the yellow module, the genes were mainly enriched in biological processes such as response to abscisic acid (GO:0009737), response to cold (GO:0009409), and hormone-mediated signaling pathways (GO:0009755) (Fig. 5B).

In the turquoise module, the genes were mainly enriched in the following: biological processes such as the abscisic acid activated signaling pathway (GO:0009738), response to jasmonic acid (GO:0009753), and response to cold (GO:0009409); molecular functions such as transcription factor activity, sequence-specific DNA binding (GO:0003700), nucleic acid-binding transcription factor activity (GO:0001071), and protein serine/threonine kinase activity (GO:0004674); and cellular components such as plasma membrane (GO:0005886), cell periphery (GO:0071944), and cell part (GO:0044464) (Fig. 5C).

In the magenta module, the genes were mainly enriched in biological processes such as regulation of cellular macromolecule biosynthetic process (GO:2000112), regulation of transcription, DNA-templated (GO:0006355) and regulation of nucleic acid-templated transcription (GO:1903506), and molecular functions such as nucleic acid binding transcription factor activity (GO:0001071), sequence-specific DNA binding (GO:0003700), zinc ion binding (GO:0008270), and transition metal ion binding (GO:0046914) (Fig. 5D).

KEGG enrichment of the four specific modules was carried out. The blue module included plant hormone signal transduction, quorum sensing, and carbon fixation in
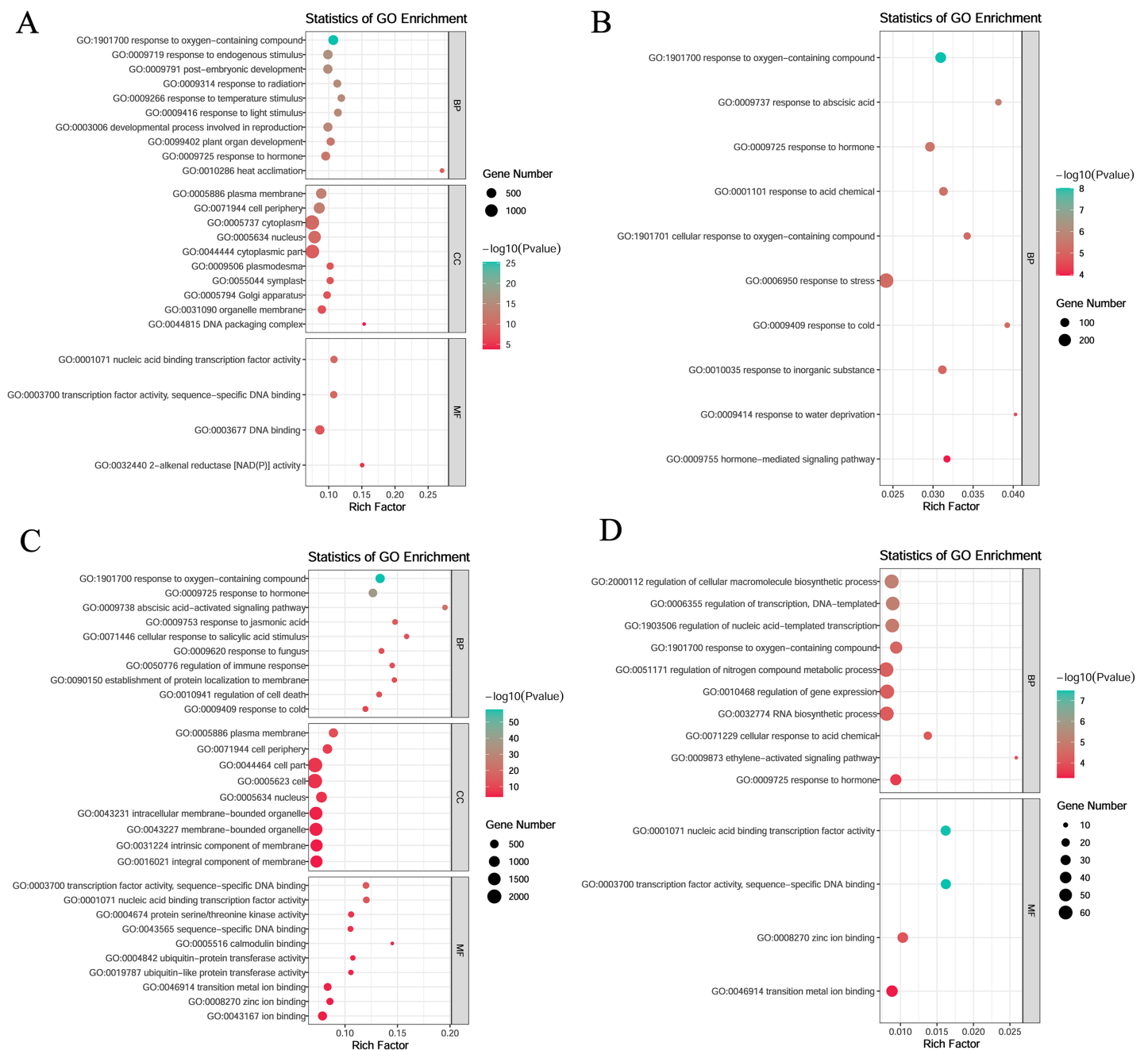
Figure 5 Gene ontology (GO) enrichment analysis of DEGs in module. (A) Blue module. (B) Yellow module. (C) Turquoise module. (D) Magenta module.

Full-size 🖼 DOI: 10.7717/peerj.19124/fig-5

photosynthetic organisms. The yellow module included plant hormone signal transduction, mitogen-activated protein kinase (MAPK) signaling pathway-plant, and vitamin B6 metabolism. The turquoise module included the MAPK signaling pathway, plant hormone signal transduction, and phenylpropanoid biosynthesis. The magenta module included plant hormone signal transduction, plant MAPK signaling pathway, and galactose metabolism (Fig. 6).
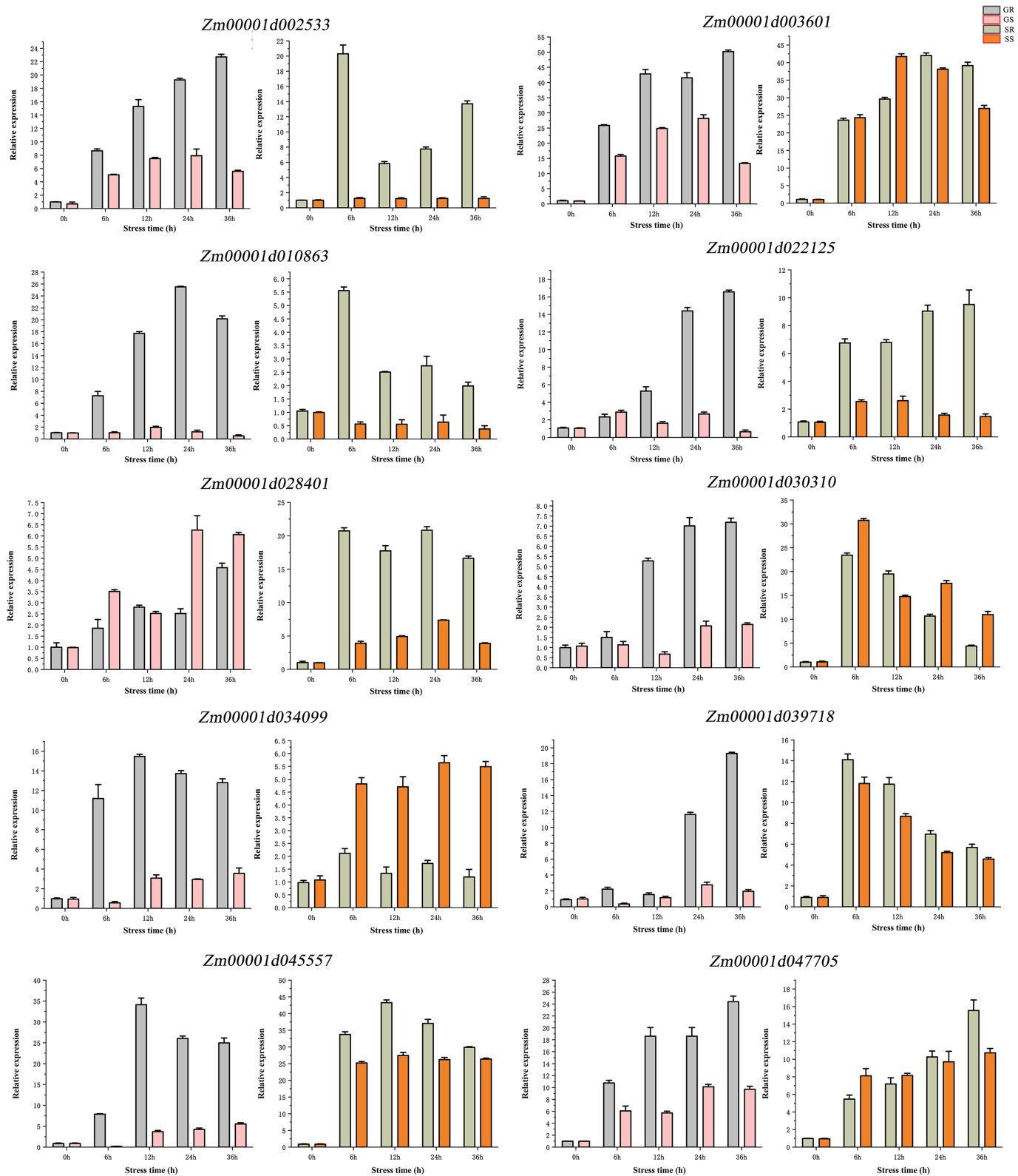
A

B

C

D
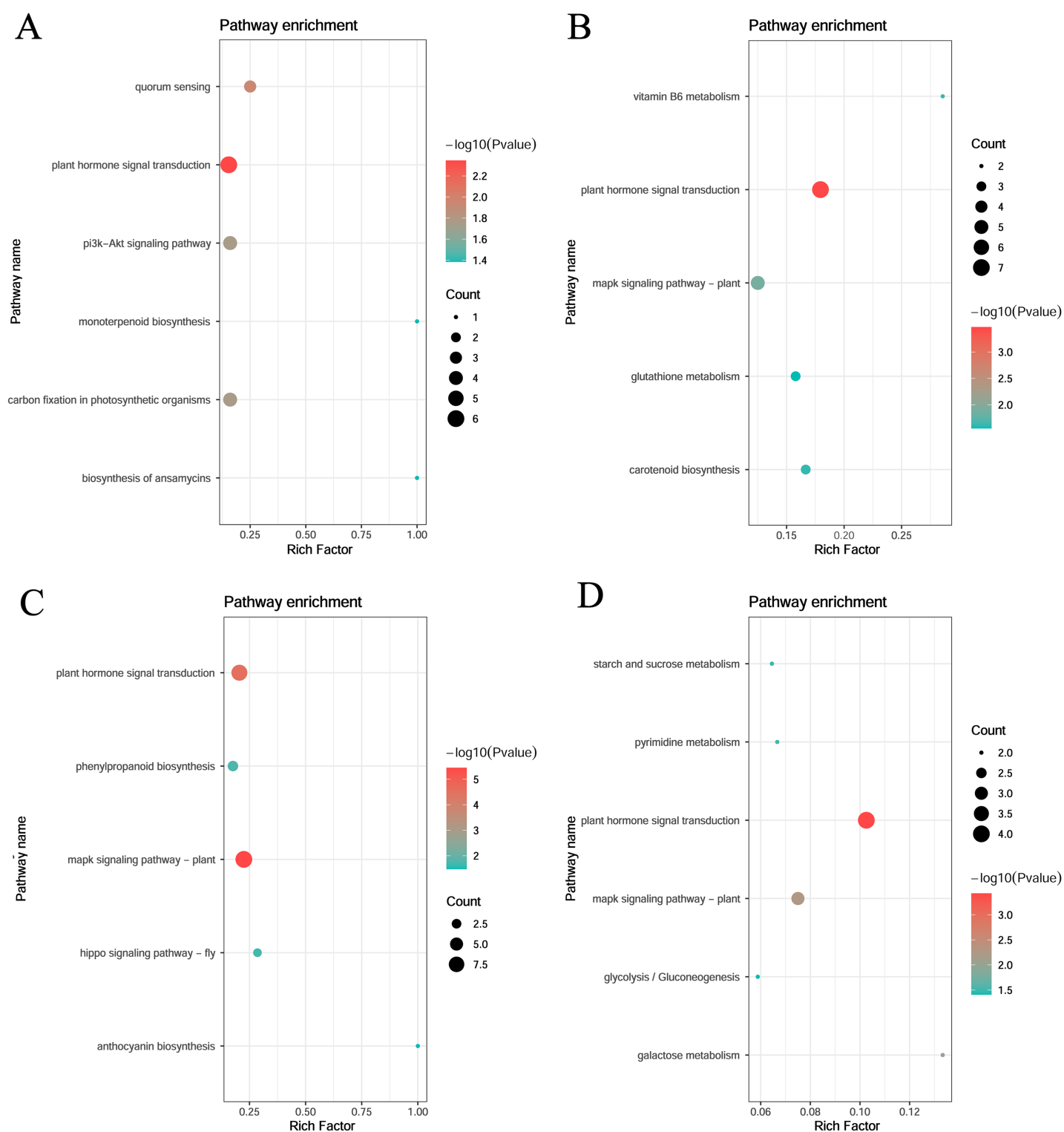
Figure 6 KEGG pathway analysis of DEGs in module. (A) Blue module. (B) Yellow module. (C) Turquoise module. (D) Magenta module.

Full-size 🖾 DOI: 10.7717/peerj.19124/fig-6

Figure 7 (A–J) qRT-PCR validation of DEGs from RNA-seq data. Abbreviations: Resistant inbred lines at the Germination stage (GR); Susceptible inbred lines at the Germination stage (GS); Resistant inbred lines at the Sprouting stage (SR); Susceptible inbred lines at the Sprouting stage (SS). Full-size ☐ DOI: 10.7717/peerj.19124/fig-7

Gene network visualization

Hub genes are typically those that have a high connectivity within a module. We selected the top 50 genes with the highest connectivity in the blue, yellow, magenta, and turquoise modules for mapping and selected the top 10 genes in terms of connectivity as hub genes. We visualized the hub genes and their associated genes and constructed a gene interaction network (Figs. S3–S5). Forty key genes including eight transcription factors tolerant to cold were predicted. Seven genes have been proven to be involved in the response to low-temperature stress (Table S1).

RT verification

qRT-PCR validation was performed for 10 genes (Fig. 7). We found that these genes have differences in their expression profiles in different lines and at different stages. The results showed that 10 candidate genes have a trend from low to high expression. At the germination stage, the expression of nine genes (except *Zm00001d028401*), was higher in the R line than in the S line, *Zm00001d010863* and *Zm00001d028401* had the highest expression at 24 h of stress, *Zm00001d034099* and *Zm00001d045557* had the highest expression at 12 h of stress, and the rest of the six genes all had the highest expression at 36 h. At the sprouting stage, the expression levels of *Zm00001d002533*, *Zm00001d010863*, *Zm00001d022125*, and *Zm00001d028401* were significantly higher in the R than in the S lines. The expression *of Zm00001d034099* was significantly higher in the S than in the R lines, and the remaining genes were not significantly different in terms of expression between the two lines. Compared with the germination stage, the gene expression at the sprouting stage showed no significant change across time. Overall, 10 genes exhibited similar expression patterns in qRT-PCR and RNA-seq experiments.

DISCUSSION

WGCNA provides new ideas and methods for resolving gene regulatory networks for different traits and has been widely used. In this study, we used WGCNA to identify four specific modules (blue, yellow, turquoise and magenta) for low-temperature tolerance in maize at the germination and sprouting stages. Through KEGG-pathway analysis of the modules and by calculating the characterized genes in these modules, we identified pathways and genes in maize that are involved in the cold stress response. The results provide new clues for further research on the molecular mechanism underlying the tolerance of maize to low-temperature stress.

KEGG pathway enrichment analysis revealed that phytohormone signaling pathways with important roles in abiotic stress were enriched in all four modules of both stages. Abscisic acid is involved in the regulation of responses to abiotic stresses including cold (*Qin et al., 2021*). Gibberellic acid is also known to play a role in plant cold tolerance and increasing endogenous biosynthesis (*Eremina, Rozhon & Poppenberger, 2016*; *Rihan, Al-Issawi & Fuller, 2017*). Salicylic acid (SA) was strongly correlated with an increase in antioxidant enzyme activities in maize seeds during seedling growth at low temperatures (*Wang et al., 2013*). Exogenous application of brassinolide also increases the germination rate, reduces cold damage to maize seedlings, and increases antioxidant enzyme activity

(*Sun et al., 2020*). The yellow, turquoise, and magenta modules were enriched in the MAPK signaling pathway. MAPKs are involved in several important processes, including stress signaling and development (*Kong et al., 2013*). The MAPK cascade pathway is a ubiquitous signaling module in eukaryotes that is regulated by changes in hormone and calcium levels. When plants experience cold stress, cytoplasmic calcium levels increase and are sensed by calcium-binding proteins, which interact with other proteins and initiate phosphorylation cascades involving major stress-responsive genes and transcription factors, leading to cold-stress tolerance. Thus, both stages may respond to cold stress by transducing cold signals *via* phytohormones and MAPKs (*Pagter et al., 2017*; *Xing et al., 2024*). Each module all had specific pathway enrichment as follows: the blue module in quorum sensing, the phosphoinositide 3-kinase-protein kinase B signaling pathway, carbon fixation in photosynthetic organisms, ansamycin biosynthesis, and monoterpene biosynthesis; the yellow module in vitamin B6 metabolism, carotenoid biosynthesis, and glutathione metabolic pathways; the turquoise module in phenylacetone biosynthesis, the Hippo signaling pathway, *Drosophila melanogaster*, and floral turquoise pigment biosynthesis; and the magenta module in galactose metabolism, pyrimidine metabolism, starch and sucrose metabolism, and glycolysis/glycogenesis pathways, which play important roles in cold stress (*Pang et al., 2021*).

Of the top 10 genes annotated to function in the four modules, seven have been shown to be associated with cold tolerance. Of these, the genes *LOC100383301* and *LOC100284949* have been cloned and validated in maize. *LOC100383301* has been annotated with calcium-dependent protein kinase family proteins, which play important roles in abiotic stress tolerance through hormone and reactive oxygen species (ROS) signaling (*Cheng et al., 2002*; *Ranty et al., 2016*). *LOC100284949* has been annotated with the bZIP transcription factor superfamily protein, which plays multiple roles in abiotic stress responses (*Baillo et al., 2019*; *He et al., 2024*; *Li et al., 2020*). The functions of *LOC100286109*, *LOC100191562*, *LOC100273668*, *LOC100282914*, and *LOC100276374* in other crops were validated. *LOC100286109* has been annotated with dehydration-responsive element-binding protein 2A (DREB2A) (*Ohama et al., 2017*). DREB2A is a key transcription factor that activates the expression of several stress-inducible genes in response to both heat and drought conditions by specifically binding to the cis-acting dehydration-responsive element/C-repeat, thereby enhancing plant tolerance to these conditions (*Liu et al., 1998*; *Sakuma et al., 2006*). *LOC100191562* annotated cytochrome P450s (CYPs) not only are involved in the biosynthesis of phytohormones and secondary metabolites but also accumulate in response to cold stress (*Chopra et al., 2015*; *Wang et al., 2009*). *LOC100273668* annotates acyl-CoA binding domain-containing proteins (ACBPs), which are involved in lipid metabolism, plant development, and abiotic stress responses (*Xiao & Chye, 2009*; *Xiao & Chye, 2011*; *Yurchenko & Weselake, 2011*). *LOC100282914* has been annotated with the RING zinc finger structural domain superfamily of proteins, RING-containing proteins that are E3 ubiquitin ligases (*Li et al., 2022*), with ubiquitinated target proteins that function in the regulation of a wide range of cellular activities, including cofactor signaling, defense signaling, and a inbred line of abiotic stress responses (*Li et al., 2011*; *Ma et al., 2009*; *Yang*

et al., 2019). *LOC100276374* annotates the WD40 family of proteins, which enable plants to respond to abiotic stress by reducing ROS and MDA levels (*Tian et al., 2023*; *Xu et al., 2019*; *Zhang et al., 2018*; *Zhang et al., 2017*). Although WGCNA was unable to truly elucidate mechanisms of genes tolerant to low-temperatures in maize at the germination and sprouting stages, it provide important clues for further research in the future.

CONCLUSIONS

We constructed a co-expression network of weighted genes related to low-temperature tolerance traits in maize. Abiotic stress regulatory pathways were found to be closely linked to some of the hub genes. These include the bZIP transcription factor superfamily protein (*LOC100284949*), the dehydration-responsive element-binding protein 2A (*LOC100286109*), the cytochrome P450 superfamily protein (*LOC100191562*), and the acyl-CoA binding protein pseudogene (*LOC100285298*). However, it is currently unclear what specific roles these genes play in the process. These results provide clues for studying the molecular mechanism underlying low-temperature tolerance in maize seedlings and provide theoretical support for the cultivation of new low-temperature-tolerant maize inbred lines.

ADDITIONAL INFORMATION AND DECLARATIONS

Competing Interests

The authors declare that they have no competing interests.

Author Contributions

- Chuangye Shi conceived and designed the experiments, performed the experiments, analyzed the data, prepared figures and/or tables, authored or reviewed drafts of the article, and approved the final draft.
- Jing Dong conceived and designed the experiments, analyzed the data, prepared figures and/or tables, and approved the final draft.
- Chunxiao Zhang conceived and designed the experiments, prepared figures and/or tables, and approved the final draft.

- Liquan Sun conceived and designed the experiments, analyzed the data, prepared figures and/or tables, and approved the final draft.
- Fengxue Jin performed the experiments, authored or reviewed drafts of the article, and approved the final draft.
- Xiaohui Zhou performed the experiments, authored or reviewed drafts of the article, and approved the final draft.
- Xueyan Liu performed the experiments, authored or reviewed drafts of the article, and approved the final draft.
- Weilin Wu conceived and designed the experiments, authored or reviewed drafts of the article, and approved the final draft.
- Xiaohui Li conceived and designed the experiments, authored or reviewed drafts of the article, and approved the final draft.

Data Availability

The following information was supplied regarding data availability:

The original measurement values are available in the Supplemental File.

Supplemental Information

Supplemental information for this article can be found online at http://dx.doi.org/10.7717/peerj.19124#supplemental-information.

REFERENCES

Allen DJ, Ort DR. 2001. Impacts of chilling temperatures on photosynthesis in warm-climate plants. *Trends in Plant Science* **6(1)**:36–42 DOI 10.1016/s1360-1385(00)01808-2.

Baillo EH, Kimotho RN, Zhang Z, Xu P. 2019. Transcription factors associated with abiotic and biotic stress tolerance and their potential for crops improvement. *Genes* **10(10)**:771 DOI 10.3390/genes10100771.

Berberich T, Sano H, Kusano T. 1999. Involvement of a MAP kinase, *ZmMPK5*, in senescence and recovery from low-temperature stress in maize. *Molecular and General Genetics* **262(3)**:534–542 DOI 10.1007/s004380051115.

Cheng SH, Willmann MR, Chen HC, Sheen J. 2002. Calcium signaling through protein kinases. The Arabidopsis calcium-dependent protein kinase gene family. *Plant Physiology* **129(2)**:469–485 DOI 10.1104/pp.005645.

Chopra R, Burow G, Hayes C, Emendack Y, Xin Z, Burke J. 2015. Transcriptome profiling and validation of gene based single nucleotide polymorphisms (SNPs) in sorghum genotypes with contrasting responses to cold stress. *BMC Genomics* **16**:1040 DOI 10.1186/s12864-015-2268-8.

Eremina M, Rozhon W, Poppenberger B. 2016. Hormonal control of cold stress responses in plants. *Cellular and Molecular Life Sciences* **73(4)**:797–810 DOI 10.1007/s00018-015-2089-6.

Greaves JA. 1996. Improving suboptimal temperature tolerance in maize—the search for variation. *Journal of Experimental Botany* **47(3)**:307–323 DOI 10.1093/jxb/47.3.307.

He L, Wu Z, Wang X, Zhao C, Cheng D, Du C, Wang H, Gao Y, Zhang R, Han J, Xu J. 2024. A novel maize F-bZIP member, *ZmbZIP76*, functions as a positive regulator in ABA-mediated abiotic stress tolerance by binding to ACGT-containing elements. *Plant Science* **341(1–2)**:111952 DOI 10.1016/j.plantsci.2023.111952.

Hussain HA, Hussain S, Khaliq A, Ashraf U, Anjum SA, Men S, Wang L. 2018. Chilling and drought stresses in crop plants: implications, cross talk, and potential management opportunities. *Frontiers in Plant Science* **9**:393 DOI 10.3389/fpls.2018.00393.

Jiang H, Shi Y, Liu J, Li Z, Fu D, Wu S, Li M, Yang Z, Shi Y, Lai J, Yang X, Gong Z, Hua J, Yang S. 2022. Natural polymorphism of *ZmICE1* contributes to amino acid metabolism that impacts cold tolerance in maize. *Nature Plants* **8(10)**:1176–1190 DOI 10.1038/s41477-022-01254-3.

Juurakko CL, Cenzo GC, Walker VK. 2021. Cold acclimation and prospects for cold-resilient crops. *Plant Stress* **2(1)**:100028 DOI 10.1016/j.stress.2021.100028.

Kong X, Pan J, Zhang D, Jiang S, Cai G, Wang L, Li D. 2013. Identification of mitogen-activated protein kinase kinase gene family and MKK-MAPK interaction network in maize. *Biochemical and Biophysical Research Communications* **441(4)**:964–969 DOI 10.1016/j.bbrc.2013.11.008.

Kong X, Pan J, Zhang M, Xing X, Zhou Y, Liu Y, Li D, Li D. 2011. ZmMKK4, a novel group C mitogen-activated protein kinase kinase in maize (*Zea mays* L.), confers salt and cold tolerance in transgenic Arabidopsis. *Plant, Cell & Environment* **34(8)**:1291–1303 DOI 10.1111/j.1365-3040.2011.02329.x.

Langfelder P, Horvath S. 2008. WGCNA: an R package for weighted correlation network analysis. *BMC Bioinformatics* **9**:559 DOI 10.1186/1471-2105-9-559.

Li H, Li L, ShangGuan G, Jia C, Deng S, Noman M, Liu Y, Guo Y, Han L, Zhang X, Dong Y, Ahmad N, Du L, Li H, Yang J. 2020. Genome-wide identification and expression analysis of bZIP gene family in *Carthamus tinctorius* L. *Scientific Reports* **10**:15521 DOI 10.1038/s41598-020-72390-z.

Li M, Lin L, Zhang Y, Sui N. 2019. *ZmMYB31*, a R2R3-MYB transcription factor in maize, positively regulates the expression of CBF genes and enhances resistance to chilling and oxidative stress. *Molecular Biology Reports* **46(4)**:3937–3944 DOI 10.1007/s11033-019-04840-5.

Li Y, Qin P, Sun A, Xiao W, Chen F, He Y, Yu K, Li Y, Zhang M, Guo X. 2022. Genome-wide identification, new classification, expression analysis and screening of drought & heat resistance related candidates in the RING zinc finger gene family of bread wheat (*Triticum aestivum* L.). *BMC Genomics* **23**:696 DOI 10.1186/s12864-022-08905-x.

Li Y, Wu B, Yu Y, Yang G, Wu C, Zheng C. 2011. Genome-wide analysis of the RING finger gene family in apple. *Molecular Genetics and Genomics* **286(1)**:81–94 DOI 10.1007/s00438-011-0625-0.

Liang T, Qing C, Liu P, Zou C, Yuan G, Pan G, Shen Y, Ma L. 2022. Joint GWAS and WGCNA uncover the genetic control of calcium accumulation under salt treatment in maize seedlings. *Physiologia Plantarum* **174(1)**:e13606 DOI 10.1111/ppl.13606.

Liu Q, Kasuga M, Sakuma Y, Abe H, Miura S, Yamaguchi-Shinozaki K, Shinozaki K. 1998. Two transcription factors, DREB1 and DREB2, with an EREBP/AP2 DNA binding domain separate two cellular signal transduction pathways in drought- and low-temperature-responsive gene expression, respectively, in Arabidopsis. *The Plant Cell* **10(8)**:1391–1406 DOI 10.1105/tpc.10.8.1391.

Liu J, Zhang CX, Li SF, Zheng DH, Liang XH, Wang Y, Liu WP, Liu XY, Cao TH, Li XH. 2021. Evaluation on chilling tolerance of ninety-five inbred lines at maize germination stage and analysis on genetic basis. *Molecular Plant Breeding* **19**:2391–2401 DOI 10.13271/j.mpb.019.002391.

Livak KJ, Schmittgen TD. 2001. Analysis of relative gene expression data using real-time quantitative PCR and the $2^{-\Delta\Delta CT}$ method. *Methods* **25(4)**:402–408 DOI 10.1006/meth.2001.1262.

Ma K, Xiao J, Li X, Zhang Q, Lian X. 2009. Sequence and expression analysis of the C3HC4-type RING finger gene family in rice. *Gene* **444(1–2)**:33–45 DOI 10.1016/j.gene.2009.05.018.

Nguyen HT, Leipner J, Stamp P, Guerra-Peraza O. 2009. Low temperature stress in maize (*Zea mays* L.) induces genes involved in photosynthesis and signal transduction as studied by suppression subtractive hybridization. *Plant Physiology and Biochemistry* **47(2)**:116–122 DOI 10.1016/j.plaphy.2008.10.010.

Ohama N, Sato H, Shinozaki K, Yamaguchi-Shinozaki K. 2017. Transcriptional regulatory network of plant heat stress response. *Trends in Plant Science* **22(1)**:53–65 DOI 10.1016/j.tplants.2016.08.015.

Pagter M, Alpers J, Erban A, Kopka J, Zuther E, Hincha DK. 2017. Rapid transcriptional and metabolic regulation of the deacclimation process in cold acclimated *Arabidopsis thaliana*. *BMC Genomics* **18**:731 DOI 10.1186/s12864-017-4126-3.

Pang Z, Chen J, Wang T, Gao C, Li Z, Guo L, Xu J, Cheng Y. 2021. Linking plant secondary metabolites and plant microbiomes: a review. *Frontiers in Plant Science* **12**:621276 DOI 10.3389/fpls.2021.621276.

Qin F, Sakuma Y, Li J, Liu Q, Li YQ, Shinozaki K, Yamaguchi-Shinozaki K. 2004. Cloning and functional analysis of a novel DREB1/CBF transcription factor involved in cold-responsive gene expression in *Zea mays* L. *Plant & Cell Physiology* **45(8)**:1042–1052 DOI 10.1093/pcp/pch118.

Qin P, Zhang G, Hu B, Wu J, Chen W, Ren Z, Liu Y, Xie J, Yuan H, Tu B, Ma B, Wang Y, Ye L, Li L, Xiang C, Li S. 2021. Leaf-derived ABA regulates rice seed development via a transporter-mediated and temperature-sensitive mechanism. *Science Advances* **7(3)**:eabc8873 DOI 10.1126/sciadv.abc8873.

Ranty B, Aldon D, Cotelle V, Galaud JP, Thuleau P, Mazars C. 2016. Calcium sensors as key hubs in plant responses to biotic and abiotic stresses. *Frontiers in Plant Science* **7(25)**:327 DOI 10.3389/fpls.2016.00327.

Rihan HZ, Al-Issawi M, Fuller MP. 2017. Advances in physiological and molecular aspects of plant cold tolerance. *Journal of Plant Interactions* **12**:143–157 DOI 10.1080/17429145.2017.1308568.

Sakuma Y, Maruyama K, Osakabe Y, Qin F, Seki M, Shinozaki K, Yamaguchi-Shinozaki K. 2006. Functional analysis of an Arabidopsis transcription factor, DREB2A, involved in drought-responsive gene expression. *The Plant Cell* **18(5)**:1292–1309 DOI 10.1105/tpc.105.035881.

Sun Y, He Y, Irfan AR, Liu X, Yu Q, Zhang Q, Yang D. 2020. Exogenous brassinolide enhances the growth and cold resistance of maize (*Zea mays* L.) seedlings under chilling stress. *Agronomy* **10**:488 DOI 10.3390/agronomy10040488.

Tian G, Wang S, Wu J, Wang Y, Wang X, Liu S, Han D, Xia G, Wang M. 2023. Allelic variation of *TaWD40-4B.1* contributes to drought tolerance by modulating catalase activity in wheat. *Nature Communications* **14(1)**:1200 DOI 10.1038/s41467-023-36901-6.

Wang X, Feng J, White PJ, Shen J, Cheng L. 2020. Heterogeneous phosphate supply influences maize lateral root proliferation by regulating auxin redistribution. *Annals of Botany* **125(1)**:119–130 DOI 10.1093/aob/mcz154.

Wang Y, Wen T, Hu J, Han R, Zhu Y-F, Guan Y, Zhu S. 2013. Relationship between endogenous salicylic acid and antioxidant enzyme activities in maize seedlings under chilling stress. *Experimental Agriculture* **49(2)**:295–308 DOI 10.1017/S0014479712001329.

Wang F, Wu H, Yang M, Xu W, Zhao W, Qiu R, Kang N, Cui G. 2024. Unveiling salt tolerance mechanisms and hub genes in Alfalfa (*Medicago sativa* L.) through transcriptomic and WGCNA analysis. *Plants* **13(22)**:3141 DOI 10.3390/plants13223141.

Wang X, Yang P, Zhang X, Xu Y, Kuang T, Shen S, He Y. 2009. Proteomic analysis of the cold stress response in the moss, Physcomitrella patens. *Proteomics* **9(19)**:4529–4538 DOI 10.1002/pmic.200900062.

Xiao S, Chye ML. 2009. An Arabidopsis family of six acyl-CoA-binding proteins has three cytosolic members. *Plant Physiology and Biochemistry* **47(6)**:479–484 DOI 10.1016/j.plaphy.2008.12.002.

Xiao S, Chye ML. 2011. New roles for acyl-CoA-binding proteins (ACBPs) in plant development, stress responses and lipid metabolism. *Progress in Lipid Research* **50(2)**:141–151 DOI 10.1016/j.plipres.2010.11.002.

Xing K, Zhang J, Xie H, Zhang L, Zhang H, Feng L, Zhou J, Zhao Y, Rong J. 2024. Identification and analysis of MAPK cascade gene families of Camellia oleifera and their roles in response to cold stress. *Molecular Biology Reports* **51(1)**:602 DOI 10.1007/s11033-024-09551-0.

Xu X, Wan W, Jiang G, Xi Y, Huang H, Cai J, Chang Y, Duan CG, Mangrauthia SK, Peng X, Zhu JK, Zhu G. 2019. Nucleocytoplasmic trafficking of the Arabidopsis WD40 repeat protein XIW1 regulates ABI5 stability and abscisic acid responses. *Molecular Plant* **12(12)**:1598–1611 DOI 10.1016/j.molp.2019.07.001.

Yang L, Miao M, Lyu H, Cao X, Li J, Li Y, Li Z, Chang W. 2019. Genome-wide identification, evolution, and expression analysis of RING finger gene family in *Solanum lycopersicum*. *International Journal of Molecular Science* **20(19)**:4864 DOI 10.3390/ijms20194864.

Yu T, Zhang J, Cao J, Ma X, Li W, Yang G. 2023. Hub gene mining and co-expression network construction of low-temperature response in maize of seedling by WGCNA. *Genes* **14(8)**:1598 DOI 10.3390/genes14081598.

Yurchenko OP, Weselake RJ. 2011. Involvement of low molecular mass soluble acyl-CoA-binding protein in seed oil biosynthesis. *New Biotechnology* **28(2)**:97–109 DOI 10.1016/j.nbt.2010.09.011.

Zeng R, Li Z, Shi Y, Fu D, Yin P, Cheng J, Jiang C, Yang S. 2021. Natural variation in a type-A response regulator confers maize chilling tolerance. *Nature Communications* **12**:4713 DOI 10.1038/s41467-021-25001-y.

Zhang B, Horvath S. 2005. A general framework for weighted gene co-expression network analysis. *Statistical Applications in Genetics and Molecular Biology* **4(1)**:17 DOI 10.2202/1544-6115.1128.

Zhang D, Wang Y, Shen J, Yin J, Li D, Gao Y, Xu W, Liang J. 2018. *OsRACK1A*, encodes a circadian clock-regulated WD40 protein, negatively affect salt tolerance in rice. *Rice* **11(1)**:45 DOI 10.1186/s12284-018-0232-3.

Zhang M, Zhang GQ, Kang HH, Zhou SM, Wang W. 2017. TaPUB1, a putative E3 ligase gene from wheat, enhances salt stress tolerance in transgenic Nicotiana benthamiana. *Plant and Cell Physiology* **58(10)**:1673–1688 DOI 10.1093/pcp/pcx101.

Zhao X, He F, Qi G, Sun S, Shi Z, Niu Y, Wu Z. 2024. Transcriptomic and physiological studies unveil that brassinolide maintains the balance of maize's multiple metabolisms under low-temperature stress. *International Journal of Molecular Sciences* **25(17)**:9396 DOI 10.3390/ijms25179396.

Zhao X, Niu Y, Hossain Z, Zhao B, Bai X, Mao T. 2023. New insights into light spectral quality inhibits the plasticity elongation of maize mesocotyl and coleoptile during seed germination. *Frontiers in Plant Science* **14**:1152399 DOI 10.3389/fpls.2023.1152399.